Supplementary Material for The Simplest and Most Predictive Model of Muon $g-2$ and Thermal Dark Matter

Ian Holst[a,b], Dan Hooper[a,b,c], and Gordan Krnjaic[a,b,c]
[a] *University of Chicago, Department of Astronomy and Astrophysics*
[b] *University of Chicago, Kavli Institute for Cosmological Physics and*
[c] *Fermi National Accelerator Laboratory, Theoretical Astrophysics Group*

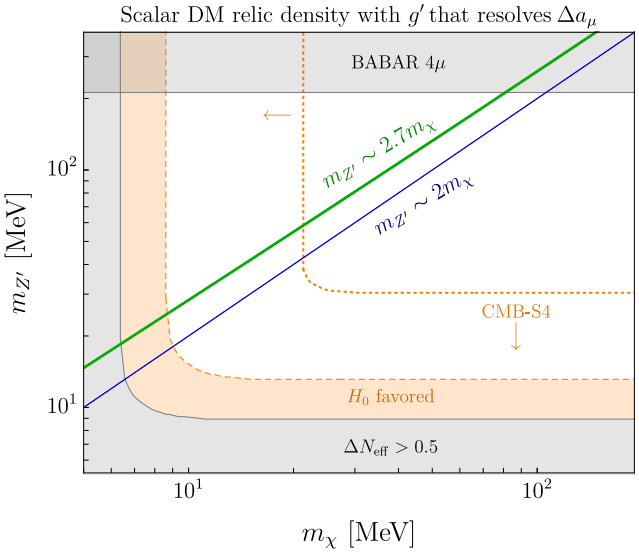

FIG. S.1. As in Fig. 3 of the main text, but for a complex scalar DM candidate instead of a Dirac fermion.

Supplementary Material: The Case of Scalar Dark Matter

In the main body of this *Letter*, we focused on the case of DM in the form of a Dirac fermion. We can similarly consider a DM candidate that is a complex scalar, ϕ, which couples to the same $L_\mu - L_\tau$ gauge boson considered above. In this case, the DM current is $J^\mu_{\rm DM} \equiv i(\phi^* \partial^\mu \phi - \phi \partial^\mu \phi^*)$, and the annihilation cross section is

$$\sigma(s) = \sum_f \frac{k_f g'^4}{12\pi s} \beta_f \, \beta_\chi \left[\frac{(s + 2m_f^2)}{(s - m_{Z'}^2)^2 + m_{Z'}^2 \Gamma_{Z'}^2} \right], \tag{S.1}$$

where the sum is over SM species $f = \mu, \tau, \nu_{\mu,\tau}$ and the total Z' width is

$$\Gamma_{Z'} = \frac{g'^2 m_{Z'}}{48\pi} \left(1 - \frac{4m_\phi^2}{m_{Z'}^2}\right)^{3/2} + \sum_f \Gamma_{Z' \to f\bar{f}}, \tag{S.2}$$

where $\Gamma_{Z' \to f\bar{f}}$ is given in Eq. 5. Unlike in the Dirac fermion scenario, here the annihilation cross section is p-wave, so annihilation during the CMB era is velocity suppressed. For scalar annihilation to e^+e^- through kinetic mixing, the non-relativistic cross section satisfies

$$\sigma v_{\phi\phi^* \to e^+e^-} \simeq \frac{(\varepsilon e g')^2 \, v^2 (m_e^2 + 2m_\phi^2) \sqrt{1 - m_e^2/m_\phi^2}}{12\pi \left[(4m_\phi^2 - m_{Z'}^2)^2 + m_{Z'}^2 \Gamma_{Z'}^2 \right]}, \tag{S.3}$$

which is further suppressed by $v^2 \ll 1$ relative to the analogous expression for Dirac DM in Eq. 13, so this scenario is not constrained by CMB bounds on $p_{\rm ann}$.

In Fig. S.1, we show the parameter space for which complex scalar DM can achieve the observed DM relic density via thermal freeze out. These results are similar to those shown in Fig. 3, but the viable parameter space is slightly shifted relative to the Dirac fermion case due to the cross section being smaller. Here the constraints based on $\Delta N_{\rm eff}$ are the same as those described in the main text, except that the contribution from DM annihilation is rescaled by a factor of 1/2 due to the difference in the number of spin degrees-of-freedom. The contribution to $\Delta N_{\rm eff}$ from Z' decays is the same as described in the main text.

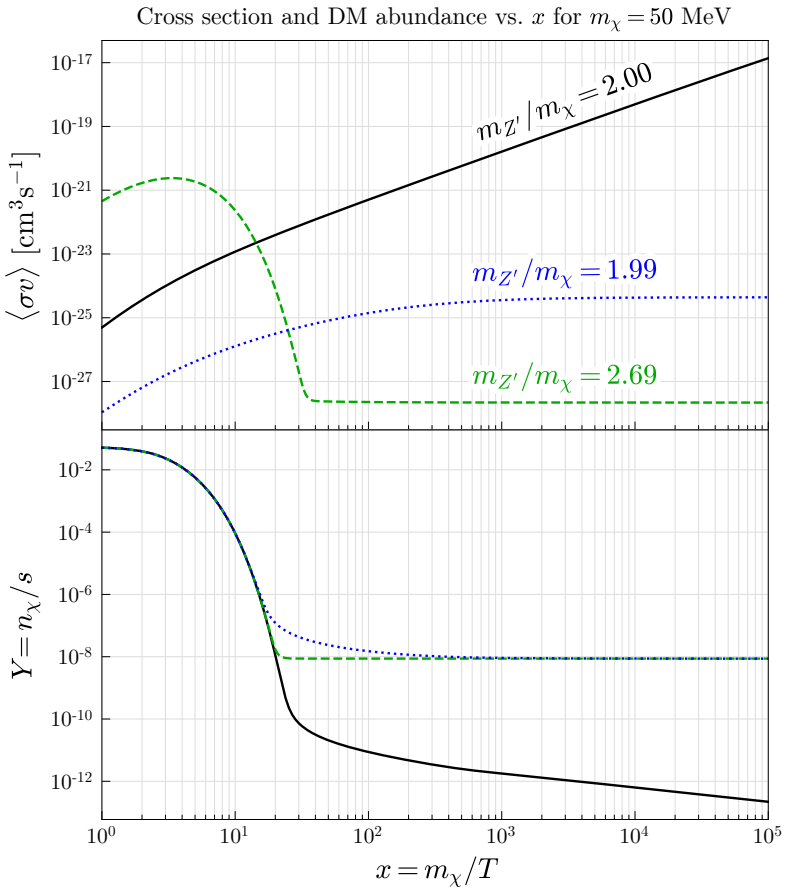

FIG. S.2. The top panel shows how the thermally averaged annihilation cross section evolves with the scaled inverse temperature, for three different mass ratios with $m_\chi = 50$ MeV. The bottom panel shows the evolution of the number density of dark matter per unit entropy from a numerical solution to the Boltzmann equation. The black (solid) line has $m_{Z'} = 2m_\chi$, while the blue (dotted) and green (dashed) lines are the two mass ratios that produce the measured dark matter density in our universe for values of g' that resolve the muon $g-2$ anomaly. Note that even though DM freeze out occurs around $x \sim 20$, the number density is severely Boltzmann suppressed *well before* freeze out. This is important because for lighter DM masses near ~ 15 MeV, freeze out actually occurs after neutrino decoupling, but this is not catastrophic because the DM population is already exponentially suppressed by $T_{\rm dec} \sim 2$ MeV even though it's still in equilibrium.

Supplementary Material: Post-Freeze Out Annihilation Near Resonance

With an approximately constant annihilation cross section, a thermal relic abundance will typically settle to its final value soon after freeze out. However, when the $m_{Z'}/m_\chi$ mass ratio is very close to 2, resonant annihilation actually becomes more efficient as the temperature decreases, leading to a significant amount of post-freeze out annihilation. Fig. S.2 illustrates this phenomenon in the solid black line, in contrast to the two other cases shown in green and blue. Note that even though the near-resonance cases result in the same final relic abundance, they take different amounts of time to reach a more stable value due to the increasing or decreasing behavior of $\langle \sigma v \rangle$ during freeze out.

In the low-velocity limit, the cross section has the following velocity dependence:

$$\sigma v \propto \frac{1}{(4 - r^2 + v^2)^2 + r^4 \gamma_{Z'}^2}, \tag{S.4}$$

where $r = m_{Z'}/m_\chi$ and $\gamma_{Z'} = \Gamma_{Z'}/m_{Z'}$. For $r \leq 2$, the cross section will increase as the velocity decreases until the two terms in the denominator are of similar magnitude, so the ultimate stopping point is controlled by the decay width. This occurs when $v \sim \sqrt{r^2 - 4 + r^2\gamma_{Z'}}$ is suppressed in the thermal distribution. Thus, post-freeze out annihilation will end earlier for $r < 2$ than for $r = 2$. For $r > 2$, the cross section will increase as the resonant peak becomes thermally favored, but then decrease and level out when typical velocities become too low to satisfy the resonance

condition. All three cases in r are illustrated in Fig. S.2. Due to this effect, one must be careful when solving the Boltzmann equation near resonance, since it may need to be integrated out to higher values of x to find acceptable convergence.